



Decolorization kinetic studies of Congo red catalyzed by Co-doped CdS nanoparticles

H.R. Pouretedal^{a*}, S.D. Mirghaderi^b, M.H. Keshavarz^a

^aFaculty of Science, Malek-Ashtaru University of Technology, Shahin-Shahr, Iran

Tel. +98 (312) 5912253; Fax +98 (312)-5220420; email: HR_POURETEDAL@mut-es.ac.ir

^bDepartment of Chemistry, Azad University, Shahreza Branch, Iran

Received 7 October 2009; Accepted in revised form 18 January 2010

ABSTRACT

The Cd_{0.97}Co_{0.03}S nanoparticles were prepared by using a controlled co-precipitation method. The nanoparticles were characterized by using UV-Vis spectra, XRD patterns and TEM image. The blue shift in the band gap of CdS semiconductor was observed with decreasing of the particle size. The XRD patterns prove the zinc-blend-type of Cd_{0.97}Co_{0.03}S nanoparticles. The size of nanoparticles less than 50 nm was confirmed through TEM image. The decolorization kinetics of Congo red catalyzed by prepared nanoparticles was studied under UV and sunlight irradiations. The decolorization study of dye with the initial concentration 20 mg/L shows the pseudo-first order kinetics with the apparent rate constant $1.35 \times 10^{-2} \text{ min}^{-1}$ at pH 7. The Cd_{0.97}Co_{0.03}S photocatalyst also indicates an excellent reactivity for bleaching of dye under sunlight irradiation with the apparent rate constant of $1.01 \times 10^{-2} \text{ min}^{-1}$. Degradation of 92–82% of Congo red was obtained in five cycles of reuse of proposed photocatalyst and dissolution of photocatalyst was found to be less than 0.2%.

Keywords: Decolorization; Cadmium sulfide; Cobalt; Nanoparticles; Congo red

1. Introduction

The removal of the non-biodegradable organic chemicals is a crucial ecological problem. Dyes are important classes of synthetic organic compounds that used in the textile industry. They are common industrial pollutants. Due to the stability of modern dyes, conventional biological treatment methods for industrial wastewater are ineffective. Heterogeneous photocatalysis by semiconductor particles is a promising technology for the reduction of global environmental pollutants. Inorganic photocatalysts such as TiO₂, ZnS, ZnO, CdS and Fe₂O₃ have shown a photocatalyst behavior for removing the

organic pollutants [1–7]. The use of photocatalysts in bleaching a variety of dyes such as methyl orange, C.I. Acid Orange 52, C.I. Basic Violet 10, Azure and Sudan dyes was reported by many researchers [8–13].

Over the past decade, the synthesis and functionalization of nanostructures have attracted great interest because of their significant potential applications. Due to the quantum confinement effect and the large surface to volume ratio, nanocrystals show very special physical and chemical properties corresponding to their bulk materials. Their sizes are close to or smaller than that of the Bohr exciton. However, the aggregation of nanocrystals always decreases their original nano-effects. During the wet chemical synthesis of nanoparticles, organic stabilizers are usually used to prevent them from aggregating by

* Corresponding author.

capping their surfaces [14]. Among these materials, CdS, one of the most important IV–VI group semiconductors, shows suitable potential in solar cells, photoelectric devices and photocatalysts [15–17]. The cadmium sulfide has band gap energy of 2.42 eV at room temperature and can be used for photoelectronic devices. In recent years, CdS nanostructural materials have been widely investigated [18–23]. Recently, several methods have been successfully applied for the preparation of CdS nanosized materials, including hydrothermal synthesis [24], microemulsion method [25], ultraviolet irradiation technology [26] and precipitation method [27].

The present work deals with the chemical co-precipitation method for preparation nanoparticles of Co-doped CdS capped by mercaptoethanol. Decolorization of Congo red (CR) dye was studied in the presence of prepared nanoparticles as photocatalyst under UV and sunlight irradiations. The dependence of dye photodegradation rate to initial dye concentration, irradiation time, amount of photocatalyst and pH of samples were also investigated.

2. Experimental

2.1. Synthesis and characterization of nanoparticles

The chloride salts of cadmium and cobalt, and sodium sulfide, all from Merck, were used for synthesis of cobalt-doped CdS nanoparticles. Double-distilled water was used to prepare the solutions.

To prepare of CdS nanoparticles, 100.0 mL solution 0.02 M of Cd²⁺ ion and 50.0 mL solution of 0.1 M mercaptoethanol (HOCH₂CH₂SH) as capping agent were added in a balloon (three-vent) on a magnetic stirrer. Then, 100.0 mL solution of 0.02 M sodium sulfide was added drop by drop using a decanter vessel under nitrogen atmosphere while the mixture was stirred vigorously at room temperature. The Cd_{1-x}Co_xS nanoparticles with X values of 0.002, 0.005, 0.01, 0.03 and 0.05 were synthesized with suitable volumes of Cd²⁺ and Co²⁺ ions solutions (0.02 M). The centrifuge with 3000–5000 rpm was used for separation of Cd_{1-x}Co_xS nanoparticles. The solvents of water and isopropyl alcohol were applied to eliminate unreacted ions and capping agent. The prepared nanoparticles were dried at 80–100°C for about 6–10 h.

The characterization of prepared nanoparticles was studied with UV-Vis spectra, XRD pattern and TEM image. An UV-Vis spectrophotometer Perkin-Elmer Lambda 2 was used for recording spectra of 10 mM of nanoparticles in isopropyl alcohol at room temperature. The atomic absorption spectrophotometer (AAS) AA-6200 Shimadzu was used to determine the real content of Co²⁺ ions in Cd_{1-x}Co_xS nanoparticles. The nitric acid 2 mol L⁻¹ was used to dissolve 0.5000 g of the prepared nanoparticles. Then, the prepared solution was diluted to the mark with distilled water in a 100-ml volumetric flask. The absorption of sample solutions and standard solu-

tions of Co²⁺ ions in range of 1–10 mg L⁻¹ was measured by using AAS. A diffractometer Bruker D8ADVANCE, Germany with anode of Cu, wavelength: 1.5406 Å (CuKα) and filter of Ni was applied for recording the XRD pattern of nanoparticles. A JEOL JEM-1200EXII transmission electron microscope (TEM) operating at 120 kV was used for characterization of the nanoparticles. The supporting grids were formvar-covered, carbon-coated, 200-mesh copper grids. The pH of the sample solutions was adjusted with adding suitable amounts of HCl and NaOH with concentrations of 1.0×10⁻² M.

2.2. Decolorization of Congo red

Congo red (C₃₂H₂₂N₆Na₂O₆S₂) was purchased from Fluka Company. Congo red is a secondary diazo dye and is water soluble, yielding a red colloidal solution with λ_{max} 510 nm at pH 7. A low pressure mercury vapor lamp (100 W) with radiation wavelength of 332 nm and light intensity 22 W/m² was used as an UV irradiation source and placed in a 5 cm diameter quartz tube with one end tightly sealed by a Teflon stopper. The lamp and the tube were then immersed in the photoreactor cell with a light path of 3.0 cm. The photoreactor cell consisted of a cylindrical Pyrex-glass cell with 1.0 L capacity, 10 cm inside diameter and 15 cm height. A water-cooled jacket on the outside of the reactor was used for temperature control at 25°C. A magnetic stirrer was used to ensure that the suspension of the photocatalyst was uniform during the course of decolorization. At regular intervals, the samples were collected, filtered through Millipore membrane filters, and centrifuged to remove the nanoparticles that existed as undissolved particles in the samples. The CR solution was stirred in dark conditions to investigate the equilibrium adsorption/desorption of the dye onto the nanoparticles.

The concentration of CR in the samples was measured at λ_{max} of 510 nm by UV-Vis spectrophotometer. The concentration of the dye was evaluated using Beer's law with respect to the initial concentration of the dye. The degradation efficiency (%D) has been calculated by Eq. (1):

$$\%D = [(C_o - C_t) / C_o] \times 100 = [(A_o - A_t) / A_o] \times 100 \quad (1)$$

where C_o and C_t are the initial concentration and the concentration of dye at time t, respectively, A_o and A_t are the initial absorbance and the absorbance of the sample at time t, respectively, and t is irradiation time of the sample.

3. Results and discussion

3.1. Characterization of nanoparticles

Fig. 1 shows the XRD pattern of Cd_{0.97}Co_{0.03}S nanosized powder. The three peaks with 2θ values of 26.6°, 47.5° and 56.4° correspond to the (1 1 1), (2 2 0) and (3 1 1) planes of the cubic phase CdS, respectively. Therefore, the dop-

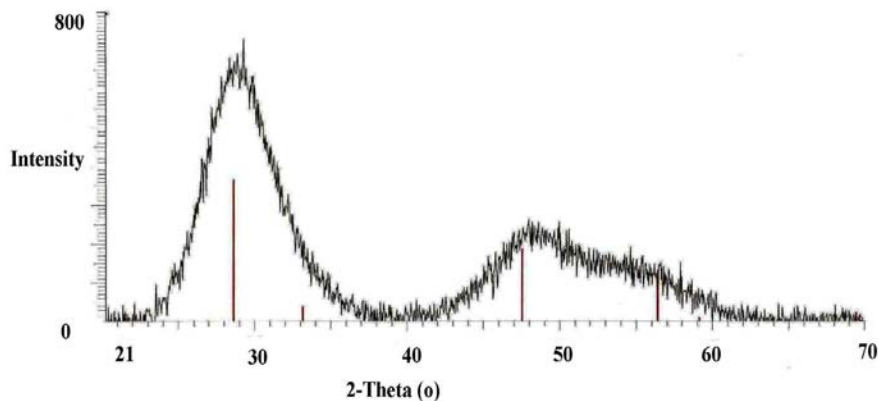


Fig. 1. X-ray diffraction pattern of $\text{Cd}_{0.97}\text{Co}_{0.03}\text{S}$ nanocrystals.

ant of cobalt did not show any considerable change in crystalline form of CdS powder. On the other hand, the broadness of the peaks in the XRD pattern can be used to confirm the formation of nanoparticles by the controlled co-precipitation method in the presence of mercaptoethanol as a capping agent. The role of mercaptoethanol is to stabilize the nanoparticles against aggregation which may lead to an increase in the size of the particles [28]. The average size of the nanoparticles powder was calculated to be about 10 nm according to Scherrer's formula [29].

The real content of Co^{2+} ions by AAS in $\text{Cd}_{0.998}\text{Co}_{0.002}\text{S}$, $\text{Cd}_{0.995}\text{Co}_{0.005}\text{S}$, $\text{Cd}_{0.99}\text{Co}_{0.01}\text{S}$, $\text{Cd}_{0.97}\text{Co}_{0.03}\text{S}$ and $\text{Cd}_{0.95}\text{Co}_{0.05}\text{S}$ was obtained 0.001, 0.004, 0.009, 0.026 and 0.047, respectively. The obtained results show that the incorporation of Co^{2+} ions in CdS lattice was down by the proposed method.

A TEM image of the prepared $\text{Cd}_{0.97}\text{Co}_{0.03}\text{S}$ nanoparticles is shown in Fig. 2. The nanoparticles have a spherical morphology with an average diameter of ca.12 nm. But moderate agglomeration is also observed due to the high surface energy of the nanoparticles. The TEM analysis also shows that the nanoparticles are sintered together and most of the nanoparticles have a slightly irregular and rounded shape.

An average diameter of 3.4 nm for the $\text{Cd}_{0.97}\text{Co}_{0.03}\text{S}$ nanoclusters was estimated from the absorption edge of 402 nm (3.1 eV) in isopropyl alcohol solvent (see Fig. 3), using Brus's effective mass model [30]. The bulk CdS peak is expected at 435 nm (2.57 eV) [18]. The blue-shifted absorption edge is due to the quantum confinement of the excitons present in the sample, resulting in a more discrete energy spectrum of the individual nanoparticles. The broadening of the absorption spectrum is mainly due to the quantum confinement of the CdS particles [19,20].

3.2. Photodegradation of Congo red

The degradation efficiencies of CR vs. time in the dark conditions and presence of CdS, under UV irradiation and



Fig. 2. TEM image of $\text{Cd}_{0.97}\text{Co}_{0.03}\text{S}$ nanoparticles.

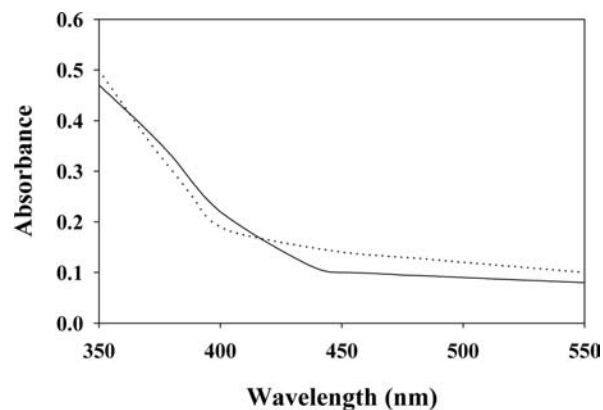


Fig. 3. UV-Vis spectra of CdS particles (solid line) and $\text{Cd}_{0.97}\text{Co}_{0.03}\text{S}$ nanoparticles (dotted line) in isopropyl solution.

absence of CdS, under UV irradiation and presence CdS and under UV irradiation and presence CdS nanoparticles are shown in Fig. 4. The UV irradiation inside the CdS particles as photocatalyst is due to the increase of degradation efficiency in a fixed time. The radiation is due to the transfer of electrons from valance band to capacitance band of CdS semiconductor and therefore, the electrons, e^- , and the holes, h^+ , are formed in valance and conductance bands, respectively. The reaction between the positive holes and the adsorbed water forms hydroxyl species. The dye degrades as non-selective to mineral species as partial or complete by hydroxyl radicals ($\cdot\text{OH}$) with $E_o = +3.06$ V as a strong oxidative [7–10,31].

Also, it is observed in Fig. 4 that the degradation efficiency increased in the presence of nanosized of CdS particles. In the semiconductor particles, the electrons excite by light absorption and therefore a high density of electrons with different kinetic energies is found in the conduction band. In the case of nanosized materials, the size of the first excited state is the same as or smaller than of the nanoparticles size. Thus, the electron and hole generated upon illumination cannot fit into such a particle unless they assume a state of higher kinetic energy. Hence, as the size of the semiconductor particle is reduced below a critical diameter, the spatial confinement of the charge carriers within a potential well like a 'particle in a box' causes them to behave quantum mechanically [32,33]. The nanoparticles with high surface area to mass ratios increase the adsorption capacities of pollutant materials and different distributions of active sites and disordered regions of the surface [33].

It is observed from Fig. 5 that with doping of CdS nanoparticles with Co^{2+} -dopant, the degradation efficiency increased in the presence of $\text{Cd}_{0.97}\text{Co}_{0.03}\text{S}$ in com-

parison to CdS nanoparticles. In other words, the CdS nanoparticles with 3% cobalt as a dopant ion has shown higher degradation efficiency of 0.2, 0.5, 1.0, 3.0 and 5.0% of cobalt-dopant. It can be concluded that the number and the lifetime of free carriers in a semiconductor depend on particle size and nature of the dopant. The dopant can serve as shallow trapping sites in a semiconductor and arrival time of electrons and holes was increased at the surface. Therefore, the increase of degradation efficiency with the increase of the dopant amount of Co^{2+} ion is expected. However, there exists an optimum Co^{2+} concentration whether the Co^{2+} acts as e^- and h^+ trap. At high concentrations, h^+ may be trapped more than once as it tries to make its way to the surface. The trapped hole can recombine with an electron before it reaches the surface and thus a photon is generated in the photocatalyst [32].

3.3. Effect of variables influence on degradation efficiency

The study of the role of pH on degradation of dyes is important because the wastewater containing them is discharged at different pHs. The obtained results from photodegradation of CR at pH range of 5.0–11.0 catalyzed by $\text{Cd}_{0.97}\text{Co}_{0.03}\text{S}$ are shown in Fig. 6. As seen from Fig. 6, the maximum degradation efficiency was obtained at pH 5–7. The pH of isoelectric point (IEP) of CdS is 7–8 and therefore the surface charge of particles is positive in acidic pH. The existence of sulfonic group in the molecule of CR is due to the negative charge of dye molecules and the increase of molecules adsorption on the surface of particles is expected. In alkaline pH's, the repulsive of CR molecules with CdS particles is due to decrease of the adsorption of dye molecules and the

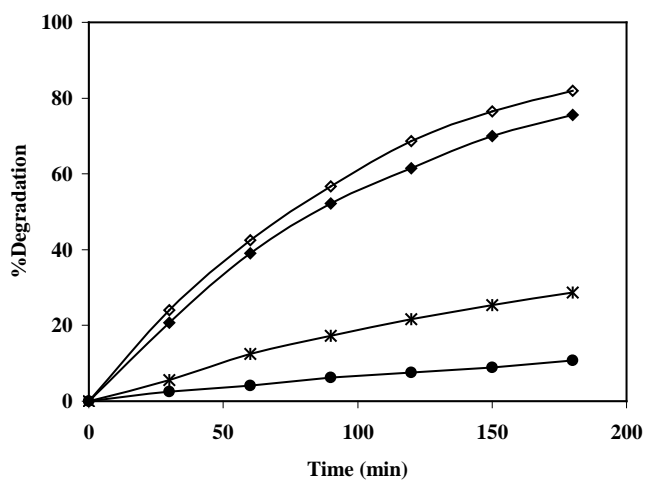


Fig. 4. The degradation efficiency vs. time in the conditions: CdS-dark (●), UV radiation (*), CdS-UV radiation (◆) and CdS nanoparticles-UV radiation (◇), CR 20.0 mg/L, catalyst 100 mg/L, pH 7 and temperature 28°C.

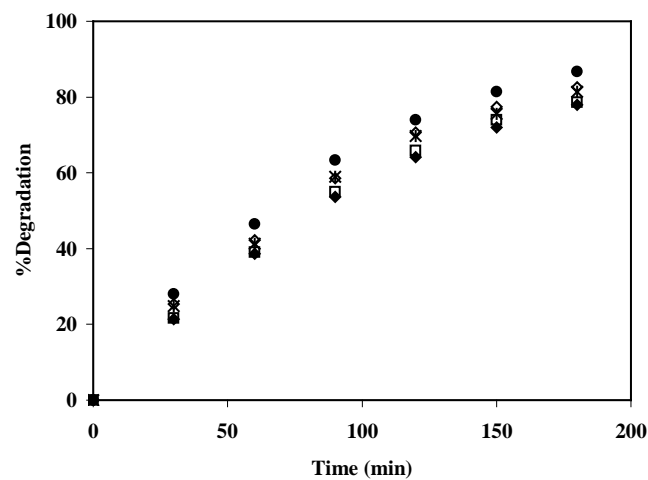


Fig. 5. The degradation efficiency vs. time in the presence of $\text{Cd}_{1-x}\text{Co}_x\text{S}$ nanoparticles; X = 0.002 (◆), 0.005 (□), 0.01 (◇), 0.03 (●) and 0.05 (*), CR 20.0 mg/L, catalyst 100 mg/L, pH 7 and temperature 28°C.

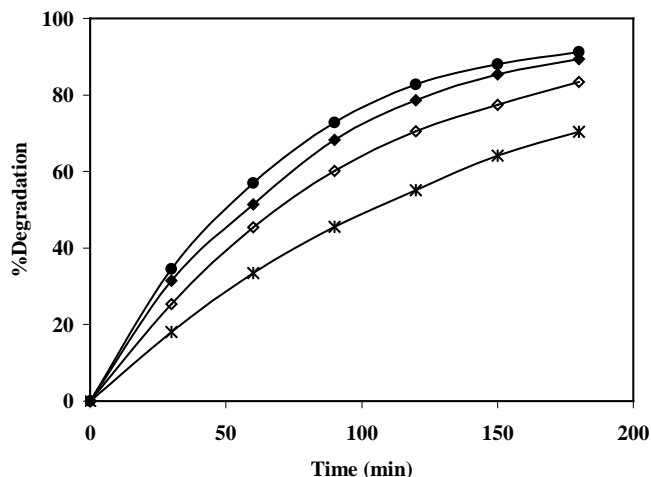


Fig. 6. Effect of sample pH on the photodegradation efficiency, pH (●) 5, (◆) 7, (◇) 9 and (*) 11, CR 20.0 mg/L, $\text{Cd}_{0.97}\text{Co}_{0.03}\text{S}$ 100 mg/L and temperature 28°C.

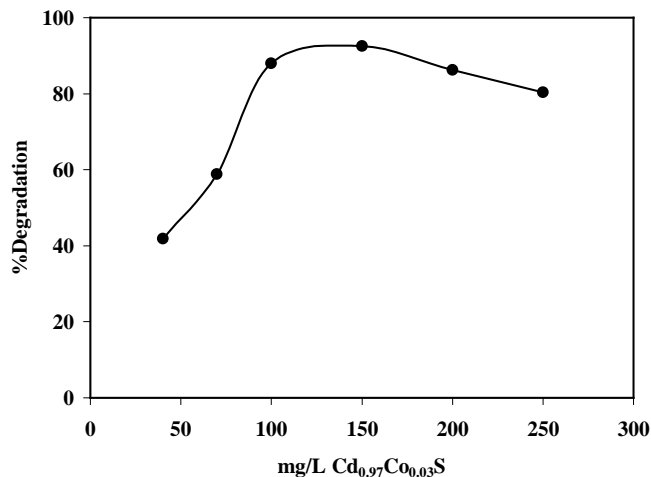


Fig. 7. Effect of dosage of $\text{Cd}_{0.97}\text{Co}_{0.03}\text{S}$ photocatalyst on the photodegradation efficiency duration 180 min, CR 20.0 mg/L, pH 7 and temperature 28°C.

decrease of degradation efficiency [34]. However, the pH 7 is selected as an optimum pH.

The degradation efficiency of Congo red (20.0 mg/L) was investigated in the range of 40–250 mg/L of $\text{Cd}_{0.97}\text{Co}_{0.03}\text{S}$ at pH 7 (Fig. 7). The results in Fig. 7 show that the photodegradation efficiency of CR was increased with increasing the amount of photocatalyst from 50 to 150 mg/L. The increasing of photocatalyst to 200 mg/L did not show any improvement in degradation efficiency and it was diminished with loading of photocatalyst above of 200 mg/L. Total active surface area and availability was increased with the increase of the photocatalyst dosage. However, as the loading was increased beyond the optimum amount, due to an increase in turbidity of the suspension with high dose of photocatalyst, there was a decrease in penetration of UV light and photoactivated volume of suspension. In these conditions, the penetration depth of the photons is decreased and less catalysts nanoparticles could be activated [35,36]. Hence, the optimum dosage of photocatalyst for degradation of CR was found 150 mg/L.

The degradation of CR was studied at different initial concentrations in the range of 5.0–30.0 mg/L. It is seen from Fig. 8 that with increasing the initial concentration of CR from 5.0 to 20.0 mg/L, the initial rate of degradation increased and then decreased above the initial concentration of 20.0 mg/L. Apparently, in high concentrations of Congo red (>20.0 mg/L) more dye molecules were adsorbed on the surface of the catalyst and thus the generation of hydroxyl radicals at the catalyst surface was reduced since the active sites were occupied by dye molecules. Moreover, as the concentration of dye increased, this also caused the dye molecules to adsorb light with the result that fewer photons could reach the

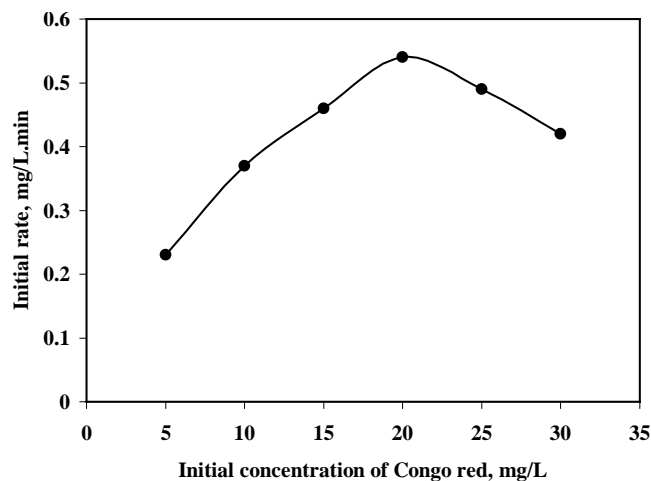


Fig. 8. Plot of initial rate of degradation versus initial concentration of CR, photocatalyst $\text{Cd}_{0.97}\text{Co}_{0.03}\text{S}$ 150 mg/L, pH 7 and temperature 28°C.

photocatalyst surface and so, photodegradation efficiency decreased [6–10,28].

3.4. Kinetic rate constants

The photocatalytic degradation of various organic compounds such as dyes catalyzed by heterogeneous photocatalysts can be formally described by the Langmuir–Hinshelwood kinetics model [37]:

$$r = dC/dt = dA/dt = kKC/(1 + KC) \quad (2)$$

For low concentrations of dyes ($KC \ll 1$), neglecting KC in the denominator and integrating with respect to

time t , the above equation can be simplified to the pseudo-first order kinetic model equation.

$$\ln(C_o / C_t) = \ln(A_o / A_t) = kKt = K_{app}t \quad (3)$$

where dC/dt is the rate of dye degradation (mg/L \times min), dA/dt is the rate of absorbance change, C is concentration of the dye (mg/L), A is absorbance of solution, t is irradiation time (min), k is reaction rate constant (min $^{-1}$), K is the adsorption coefficient of the dye onto the photocatalyst particle (L/mg) and k_{app} is the apparent rate constant calculated from the curves (min $^{-1}$). If pseudo-first order kinetic model is applicable, the plot of $\ln(C_o/C_t)$ or $\ln(A_o/A_t)$ against t in Eq. (3) should give a linear relationship, from which k_{app} can be determined from the slope of the plot. This kinetic model was applied to the experimental data and apparent rate constants of degradation at different initial concentrations of Congo red (Fig. 9), k_{app} were determined from the slope of the plots. The results are given in Table 1. Also, the half-life time at different initial concentrations of dye are reported in Table 1. As seen from Table 1, the half-life time of dye was increased with increasing the initial concentration of Congo red.

Table 1

The rate constant (k), standard deviation ($n = 3$) and half-life time of decolorization at different initial concentrations of CR, photocatalyst Cd_{0.97}Co_{0.03}S 150 mg/L, pH 7 and temperature 28°C

CR, mg/L	k , min $^{-1}$	$t^{1/2}$, min
5	$2.01 \pm 0.04 \times 10^{-2}$	34.48
10	$1.66 \pm 0.03 \times 10^{-2}$	41.75
15	$1.47 \pm 0.05 \times 10^{-2}$	47.14
20	$1.35 \pm 0.05 \times 10^{-2}$	51.33
25	$1.02 \pm 0.14 \times 10^{-2}$	67.94
30	$0.78 \pm 0.03 \times 10^{-2}$	88.85

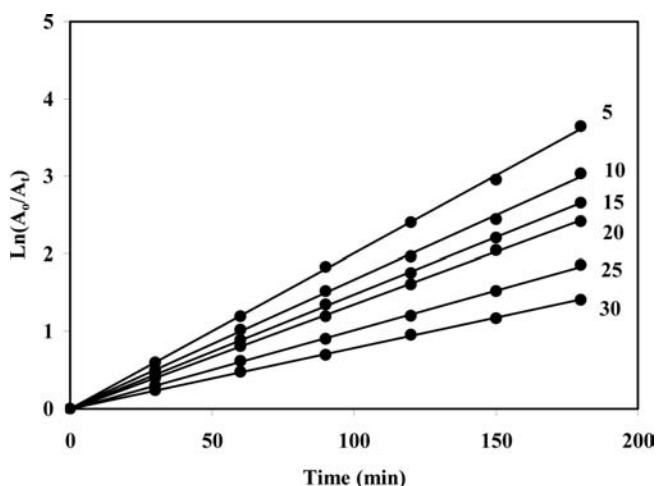


Fig. 9. Plot of $\ln(A_o/A_t)$ vs. time at different initial concentrations of dye (mg/L), photocatalyst Cd_{0.97}Co_{0.03}S 150 mg/L, pH 7 and temperature 28°C.

3.5. Reproducibility of the photocatalyst behavior

The degradation efficiency of Congo red during the five cycles of batch experiments is shown in Fig. 10. In each step of cycle experiments, the solution of the dye was filtered, washed and the photocatalyst was dried. The dried catalyst was used for the degradation of the dye under similar conditions. The decrease of degradation yield of CR after five cycles was found to be 10%. Also, the filtrate solutions were analyzed by AAS to assess the loss of Cd²⁺ ions to solutions as a result of dissolution of photocatalyst. It was observed that after the five cycles of experiments, dissolution of photocatalyst was found less than 0.2%.

3.6. Photodegradation of dye under sunlight irradiation

Utilization of sunlight as the UV energy source is beneficial from ecological point of view. Sunlight irradiation is safe and cost effective source for photocatalytic excitation and ultimately for degradation of pollutants although it has only 5% of optimum energy. Thus, in order to study the photoreactivity of Cd_{0.97}Co_{0.03}S catalyst under sunlight irradiation, photodegradation of CR was performed in spring season and in optimized conditions of 150 mg/L of photocatalyst, 20.0 mg/L Congo red at pH of 7. The decolorization efficiency of dye was obtained 43.6, 71.2, 86.2 and 90.3% after 60, 120, 180 and 240 min, respectively, with apparent rate constant of 1.01×10^{-2} min $^{-1}$. The obtained results are not surprising with the existence the absorption edge of Cd_{0.97}Co_{0.03}S semiconductor in the visible range of radiation.

3.7. Bleaching of Congo red in real water

The bleaching of dye was studied in real water containing HCO₃⁻, CO₃²⁻ and SO₄²⁻ with concentrations of 148.5,

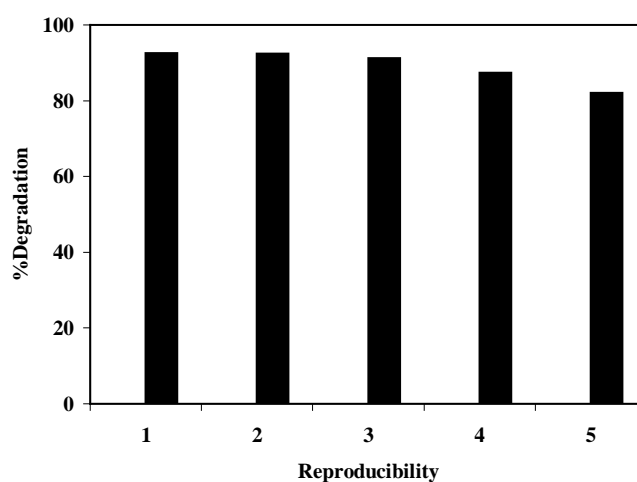


Fig. 10. Reproducibility of photoactivity of Cd_{0.97}Co_{0.03}S (150 mg/L) on the degradation of CR (20 mg/L) at pH 7 and temperature 28°C.

93.4 and 142.8 mg/L, respectively, at optimum conditions under sunlight irradiation. The degradation efficiency was obtained 74.5% after 240 min. The decrease of %D in real water in comparison with distilled water is undoubtedly due to ability of anions of bicarbonate, carbonate and sulfate as hydroxyl radical's scavengers [38]. The anions can be blocked the active sites on the surface of photocatalyst particles and therefore, the photocatalyst deactivated for pollutant molecules.

4. Conclusions

A co-precipitation method can be used for preparation of $\text{Cd}_{0.97}\text{Co}_{0.03}\text{S}$ semiconductor as nanosized powder. The prepared nanoparticles can be used as a photocatalyst for degradation process of Congo red under UV and sunlight irradiations in synthetic and real water samples. The pseudo-first order kinetic for degradation reactions was proven using the kinetic studies. The proposed photocatalyst shows good reproducibility in five cycles of degradation.

References

- [1] E.J. Weber and V.C. Stickney, Hydrolysis kinetics of reactive blue 19-vinylsulfone, *Water Res.*, 27 (1993) 63–67.
- [2] N. Guetta and H.A. Amar, Photocatalytic oxidation of methyl orange in presence of titanium dioxide in aqueous suspension. Part I: parametric study, *Desalination*, 185 (2005) 427–437.
- [3] M. Saquib and M. Muneer, Titanium dioxide mediated photocatalyzed degradation of a textile dye derivative, acid orange 8, in aqueous suspensions, *Desalination*, 155 (2003) 255–263.
- [4] K. Vinodgopal, I. Bedja, S. Hotchandani and P.V. Kamat, A photocatalytic approach for the reductive decolorization of textile azo dyes in colloidal semiconductor suspensions, *Langmuir*, 10 (1994) 767–771.
- [5] K. Vinodgopal and P.V. Kamat, Photochemistry of textile azo dyes. Spectral characterization of excited state, reduced and oxidized forms of acid orange 7, *J. Photochem. Photobiol. A*, 83 (1994) 141–146.
- [6] A. Mills, A. Belghazi, R.H. Davies, D. Worsley and S. Morris, A kinetic study of the bleaching of rhodamine 6G photosensitized by titanium dioxide, *J. Photochem. Photobiol. A*, 79 (1994) 131–139.
- [7] M. Vautier, C. Guillard and J.M. Herrmann, Photocatalytic degradation of dyes in water: case study of indigo and of indigo carmine, *J. Catal.*, 201 (2001) 46–59.
- [8] C. Chen, Z. Wang, S. Ruan, B. Zou, M. Zhao and F. Wu, Photocatalytic degradation of C.I. Acid Orange 52 in the presence of Zn-doped TiO_2 prepared by a stearic acid gel method, *Dyes Pigments*, 77 (2008) 204–209.
- [9] C.-C. Wang, C.-K. Lee, M.-D. Lyu and L.-C. Juang, Photocatalytic degradation of C.I. Basic Violet 10 using TiO_2 catalysts supported by Y zeolite: An investigation of the effects of operational parameters, *Dyes Pigments*, 76 (2008) 817–824.
- [10] T. Aarthi, P. Narahari and G. Madras, Photocatalytic degradation of Azure and Sudan dyes using nano TiO_2 , *J. Hazard. Mater.*, 149 (2007) 725–734.
- [11] I. Arslan, I.A. Balcioglu and D.W. Bahnemann, Advanced chemical oxidation of reactive dyes in simulated dyehouse effluents by ferrioxalate-Fenton/UV-A and TiO_2 /UV-A processes, *Dyes Pigments*, 47 (2000) 207–218.
- [12] S. Sakthivel, B. Neppolian, B. Arabindoo, M. Palanichamy and V. Murugesan, ZnO/UV mediated photocatalytic degradation of acid green 16, a commonly used leather dye, *Indian J. Eng. Mater. Sci.*, 7 (2000) 87–93.
- [13] J.C. Zhao, T.X. Wu, K.Q. Wu, K. Oikawa, H. Hidaka and N. Serpone, Photoassisted degradation of dye pollutants. 3. Degradation of the cationic dye rhodamine B in aqueous anionic surfactant/ TiO_2 dispersions under visible light irradiation: evidence for the need of substrate adsorption on TiO_2 particles, *Environ. Sci. Technol.*, 32 (1998) 2394–2400.
- [14] R.S. Mane and C.D. Lokhande, Chemical deposition method for metal chalcogenide thin films, *Mater. Chem. Phys.*, 65 (2000) 1–31.
- [15] A. Olea and P.J. Sebastian, (Zn,Cd)S porous layers for dye-sensitized solar cell application, *Sol. Energy Mater. Sol. Cells*, 55 (1998) 149–156.
- [16] M.M. Soliman, M.M. Shaban and F. Abulfotuh, CdS/CdTe solar cell using sputtering technique, in: Proc. IV World Renewable Energy Congress (WREC), USA, 1996. p. 386.
- [17] W.Z. Tang and C.P. Huang, Inhibitory effect of thioacetamide on CdS dissolution during photocatalytic oxidation of 2,4-dichlorophenol, *Chemosphere*, 30 (1995) 1385–1399.
- [18] H. Tang, M. Yan, H. Zhang, M. Xia and D. Yang, Preparation and characterization of water-soluble CdS nanocrystals by surface modification of ethylene diamine, *Mater. Lett.*, 59 (2005) 1024–1027.
- [19] J. Zhang, X. Yang, D. Wang, S. Li, Y. Xie, Y. Xia and Y. Qian, Polymer-controlled growth of CdS nanowires, *Adv. Mater.*, 12 (2000) 1348–1351.
- [20] D. Xu, Y. Xu, D. Chen, G. Guo, L. Gui and Y. Tang, Preparation of CdS single-crystal nanowires by electrochemically induced deposition, *Adv. Mater.*, 12 (2000) 520–522.
- [21] K. Liu, J.Y. Zhang, X. Wu, B. Li, B. Li, Y. Lu, X. Fan and D. Shen, Fe-doped and (Zn, Fe) co-doped CdS films: Could the Zn doping affect the concentration of Fe^{2+} and the optical properties, *Physica B*, 389 (2007) 248–251.
- [22] P. Zhang and L. Gao, Synthesis and characterization of CdS nanorods via hydrothermal microemulsion, *Langmuir*, 19 (2003) 208–210.
- [23] H. Zhang, X. Ma, J. Xu, J. Niu, J. Sha and D. Yang, Directional CdS nanowires fabricated by chemical bath deposition, *J. Cryst. Growth*, 246 (2002) 108–112.
- [24] G.Q. Xu and B. Liu, Luminescence studies of CdS spherical particles via hydrothermal synthesis, *J. Phys. Chem. Solids*, 61 (2000) 829–836.
- [25] A. Agostiano, M. Catalano, M.L. Curri, M. Della Monica, L. Manna and L. Vasanelli, Synthesis and structural characterisation of CdS nanoparticles prepared in a four-components "water-in-oil" microemulsion, *Micron*, 31 (2000) 253–258.
- [26] S.D. Wu and Z. Zhu, Preparation of the CdS semiconductor nanofibril by UV irradiation, *Mater. Sci. Eng. B*, 90 (2002) 206–208.
- [27] H.R. Pouretedal, M.H. Keshavarz, M.H. Yosefi, A. Shokrollahi and A. Zali, Treatment of HMX and RDX in wastewater using photodegradation process in the presence of CdS:Cu nanophotocatalyst, *Chinese J. Energ. Mater.*, 16 (2008) 745–752.
- [28] H. R. Pouretedal, A. Norozi, M.H. Keshavarz and A. Semnani, Nanoparticles of zinc sulfide doped with manganese, nickel and copper as nanophotocatalyst in the degradation of organic dyes, *J. Hazard. Mater.*, 162 (2009) 674–681.
- [29] A. Guinier, X-ray Diffraction, San Francisco, CA, 1963.
- [30] J.M. Nedeljkovic, R.C. Patel, P. Kaufman, C. Joyce-Pruden and N.O. Leary, Synthesis and optical properties of quantum-sized metal sulfide particles in aqueous solution, *J. Chem. Educ.*, 70 (1993) 342–345.
- [31] M. Qamar, M. Saquib and M. Muneer, Titanium dioxide mediated photocatalytic degradation of two selected azo dye derivatives, chrysoidine R and acid red 29 (chromotrope 2R), in aqueous suspensions, *Desalination*, 186 (2005) 255–271.
- [32] K. Dhermendra, J. Tiwari, J. Behari and P. Sen, Application of

- nanoparticles in waste water treatment, *World Appl. Sci. J.*, 3 (2008) 417–433.
- [33] D. Beydoun, R. Amal, G. Low and S. McEvoy, Role of nanoparticles in photocatalysis, *J. Nanoparticle. Res.*, 1 (1999) 439–458.
- [34] C. Ge, M. Xu, J. Fang, J. Lei and H. Ju, Luminescent cadmium sulfide nanochains templated on unfixed deoxyribonucleic acid and their erectal alignment by droplet dewetting, *J. Phys. Chem. C*, 112 (2008) 10602–10608.
- [35] H.R. Pouretedal, H. Eskandari, M.H. Keshavarz and A. Semnani, Photodegradation of organic dyes using nanoparticles of cadmium sulfide doped with manganese, nickel and copper as nanophotocatalyst, *Acta Chim. Slov.*, 56 (2009) 353–361.
- [36] M.R. Hoffmann, S.T. Martin, W. Choi and D.W. Bahnemann, Environmental applications of semiconductor photocatalysis, *Chem. Rev.*, 95 (1995) 69–85.
- [37] H. Al-Ekabi and N. Serpone, Kinetic studies in heterogeneous photocatalysis, *J. Phys. Chem.*, 92 (1988) 5726–5731.
- [38] O. Legrini, E. Oliveros and A.M. Braun, Photochemical process for water treatment, *Chem. Rev.*, 93 (1993) 671–698.